

Positive cross correlations of noise in superconducting hybrid structures: Roles of interfaces and interactions

R. Mélin,¹ C. Benjamin,^{2,3} and T. Martin^{2,4}¹*Institut NEEL, CNRS and Université Joseph Fourier, BP 166, F-38042 Grenoble Cedex 9, France*²*Centre de Physique Théorique, Case 907 Luminy, 13288 Marseille cedex 9, France*³*Quantum Information Group, School of Physics and Astronomy, University of Leeds, Woodhouse Lane, Leeds, LS29JT, United Kingdom*⁴*Université de la Méditerranée, 13288 Marseille Cedex 9, France*

(Received 3 August 2007; revised manuscript received 16 January 2008; published 13 March 2008)

Shot noise cross-correlations in normal metal–superconductor–normal metal structures are discussed at arbitrary interface transparencies using both the scattering approach of Blonder, Tinkham, and Klapwijk and a microscopic Green’s function approach. Surprisingly, negative crossed conductance in such setups [R. Mélin and D. Feinberg, *Phys. Rev. B* **70**, 174509 (2004)] does not preclude the possibility of positive noise cross-correlations for almost transparent contacts. We conclude with a phenomenological discussion of interactions in the one-dimensional leads connected to the superconductor, which induce sign changes in the noise cross-correlations.

DOI: [10.1103/PhysRevB.77.094512](https://doi.org/10.1103/PhysRevB.77.094512)

PACS number(s): 74.50.+r, 74.45.+c, 74.40.+k, 74.78.Na

I. INTRODUCTION

Among the challenges in condensed matter systems at the nanoscale is the manipulation of electronic entanglement in connection with quantum-information processing. Some theoretical proposals^{1–4} involving superconductivity have been implemented by three groups,^{5–7} aiming at the observation of nonlocal effects in transport, and in the long run at the realization of a source of entangled pairs of electrons. The devices realized up to now^{5–7} consist of ferromagnet–superconductor–ferromagnet (F_aSF_b) and normal metal–superconductor–normal metal (N_aSN_b) three-terminal hybrids, designed in such a way that Cooper pairs from the superconductor have the opportunity to split in the two different normal ($N_{a,b}$) or ferromagnetic ($F_{a,b}$) electrodes. Noise measurements, on the other hand, have focused mostly on two-terminal devices such as a two dimensional electron gas–superconductor junction⁸ and a junction between a diffusive normal metal and superconductor.⁹

The possibility of separating pairs of electrons into different electrodes^{10,11} has aroused a considerable theoretical interest recently, and calls for a new look at fundamental issues related to nonlocal transport through a superconductor, namely tunneling in three-terminal configurations in the presence of a condensate.^{12–18,20–27} In most of the above studies of three-terminal hybrids, the leads are separately connected to the source of Cooper pairs (the superconductor). Some early proposals considered a normal metal “fork” with two leads each connected to voltage probes, and with the third lead connected to a superconductor. There, the motivation was to compute the current noise cross-correlations between the two normal leads, and to see whether the sign of this signal would be reversed compared to the negative noise cross-correlations of a normal metal three-terminal device (the fermionic analog of the Hanbury Brown and Twiss experiment). Reference 28 considered a ballistic fork with an electron beam splitter, and found that positive noise correlations could arise upon reducing the transparency of the superconductor interface. Reference 13 considered a chaotic cavity connected to the superconductor

and to the leads, and found positive noise correlations which are enhanced by the backscattering of the contacts, and are robust when the proximity effect in the dot is destroyed by an external magnetic field. Positive correlations may also occur in the absence of correlated injection.²⁹

It was shown already^{2,3} that noise cross-correlations between the currents in different electrodes can lead in the long term to Einstein, Podolsky, Rosen experiments with electrons, being massive particles. In the short term, current-current correlations among electrodes N_a and N_b in N_aSN_b three-terminal structures may lead to detailed informations about the microscopic processes mediating nonlocal transport. A spin-up electron from electrode N_b may be transmitted as a spin-up electron in electrode N_a across the superconductor (a channel called as “elastic cotunneling”), or it may be transmitted as a spin-down hole in electrode N_a with a pair left in the superconductor (a channel called as “crossed Andreev reflection”) (see Fig. 1). However, in N_aSN_b structures with tunnel contacts, the elastic cotunneling current of spin-up electrons in electrode N_a turns out to be opposite to the crossed Andreev reflection current of spin-down holes in electrode N_a : As shown by Falci *et al.*¹² the lowest order contribution to the crossed conductance is vanishingly small in a N_aISIN_b structure, where an insulating layer I is supposed to be inserted in between the normal and superconducting electrodes. A finite crossed conductance is however restored to next orders in the tunnel amplitudes,^{20,23,24} if the normal electrodes $N_{a,b}$ are replaced by ferromagnets¹² $F_{a,b}$, or if interactions in the superconductor are taken into account.²²

We are motivated by the fact that contacts with moderate to large interface transparency may be used in future experiments in order to maximize the measured current noise signal. A relevant question is then the following: Do basic properties such as the sign of current cross-correlations depend or not on interface transparency, as compared to lowest order perturbation theory in the tunnel amplitudes discussed by Bignon *et al.*?³⁰ Interestingly, we obtain below a positive answer to this question, using two complementary approaches: the scattering approach of Blonder Tinkham and

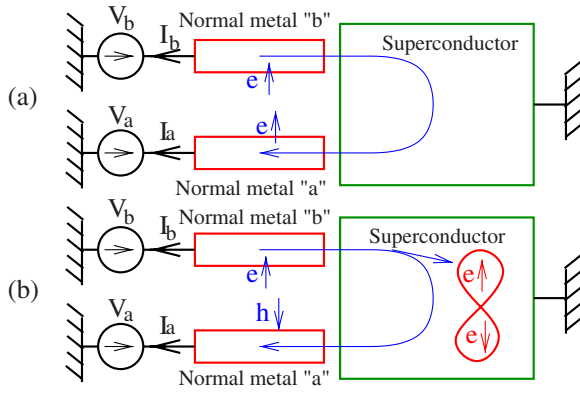
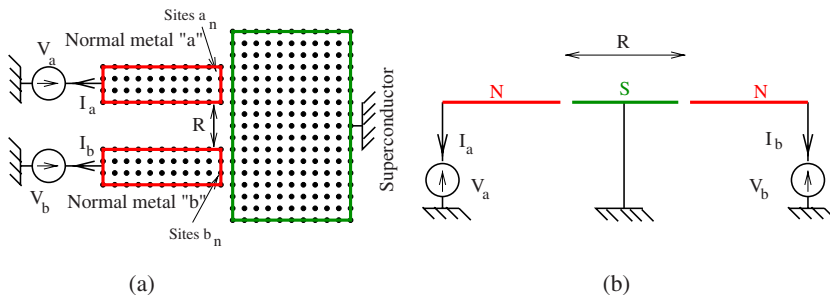


FIG. 1. (Color online) Schematic representation of elastic cotunneling (a) in a N_aSN_b structure, in which a spin-up electron ($e\uparrow$) tunnels from electrode N_b to electrode N_a across the superconductor. (b) Crossed Andreev reflection in which a spin-up electron ($e\uparrow$) coming from the normal electrode N_b is converted as a hole in the spin-down band ($h\downarrow$) in electrode N_a while a pair is transferred in the superconductor. The balance between (a) and (b) can be controlled by the relative spin orientation if the normal metals $N_{a,b}$ are replaced by ferromagnets $F_{a,b}$. The voltage V_a is set to zero in the available crossed conductance experiments (Refs. 5–7). We evaluate in the article cross-correlations between the currents I_a and I_b in the presence of arbitrary voltages V_a and V_b in the normal or ferromagnetic electrodes (Ref. 30).

Klapwijk as well as a microscopic tight binding scheme using the Keldysh method. The two approaches differ in the way interfaces are treated. The scattering approach assumes that the N_aSN_b system has a single mode connected throughout, while in the Green's function approach the local tunneling term connects “many” modes in the leads to “many” other modes in the superconductor. The study of these two limits is necessary to establish the robustness of the positive noise cross-correlation signal discussed in this paper. As we shall see, we find qualitative agreement between the two approaches.

Concerning the nonlocal conductance calculation, the situation is summarized rapidly. It was shown already^{20,23,24} that the nonlocal conductance of a N_aSN_b structure is *negative* for transparent interfaces. This was interpreted in terms of the next higher order process in the tunnel transparencies²³ corresponding to the cotunneling of pairs from electrode N_b to electrode N_a . Such processes is not expected to result in entanglement in between the two electrodes N_a and N_b because no Cooper pair from the superconductor is split between the normal electrodes N_a and N_b .



However, noise cross correlations constitutes a quantity which is distinct from the nonlocal conductance, and, surprisingly, we show that the corresponding noise cross-correlations of highly transparent N_aSN_b structures are *positive* in spite of *negative* nonlocal conductance. This is confirmed by keeping track of the processes contributing to the noise cross-correlations in the Anantram and Datta¹⁸ formula for the noise in multiterminal superconducting hybrids.

Finally, we mention that for experimental and practical reasons, the calculations presented in this paper are performed with the assumption that the distance which separates the two normal metal–superconductor interfaces is comparable or larger than the superconducting coherence length. Indeed, all experiments carried out so far for the nonlocal conductance^{5–7} have been performed within this range of parameters. For the BTK approach, this condition is necessary in order to avoid the meaningless situation where all dimensions of the superconductor are smaller than the coherence length. In the Green's function approach, lateral contacts can be at a distance smaller than the coherence length while all dimensions of the superconductor are much larger than the coherence length. We verified carefully that our results are also valid in this situation.

The article is organized as follows. Preliminaries for the Green's function and for the BTK approach are presented in Sec. II. The results of the two methods are discussed in Sec. III. Interactions in the normal metal leads are addressed in Sec. IV.

II. PRELIMINARIES

A. Noise cross-correlations

The noise cross-correlation is given by the current fluctuations

$$\mathcal{S}_{a,b}(t,t') = \langle \delta I_a(t+t') \delta I_b(t) \rangle, \quad (1)$$

where $I_a(t+t')$ and $I_b(t)$ are the currents through the normal electrodes $N_{a,b}$ (or ferromagnetic electrodes $F_{a,b}$) (see the notations “a” and “b” on Figs. 1 and 2) at times $t+t'$ and t , respectively. The current operator at time t is defined as

$$I_a(t) = t_{a,\alpha} \sum_{\sigma} \sum_n c_{\alpha_n,\sigma}^+(t) c_{a_n,\sigma}(t) + \text{H.c.}, \quad (2)$$

where H.c. is the Hermitian conjugate, $\langle \dots \rangle$ denotes a quantum mechanical expectation value, $c_{a_n,\sigma}(t)$ destroys a spin- σ electron at time t and site “ a_n ” and $c_{\alpha_n,\sigma}^+(t)$ creates a spin- σ electron at time t and site “ α_n ” (see Fig. 2 for the set of

FIG. 2. (Color online) (a) Schematic representation of the tight-binding model of N_aSN_b structure with lateral contacts used in Green's function calculations and (b) of the one dimensional (1D) N_aSN_b structure used in the BTK approach.

tight-binding sites labeled by a_n , and for their counterpart α_n in the superconducting electrode).

For dc bias applied to the electron reservoirs, time translational invariance imposes that the real time cross-correlation $\mathcal{S}_{a,b}(t_2-t_1)$ depends only on the difference of times of the two current operators. This correlator is related in a standard fashion to the Green's functions^{31,32} $\hat{G}^+(t_2-t_1)$ and $\hat{G}^-(t_2-t_1)$ connecting the two branches of the Keldysh contour:

$$\begin{aligned} \mathcal{S}_{a,b} = & \left(\frac{e}{\hbar}\right)^2 \text{Tr}[-\hat{G}_{b,\alpha}^+ \otimes \hat{t}_{\alpha,a} \otimes \hat{G}_{a,\beta}^- \otimes \hat{t}_{\beta,b} + \hat{G}_{\beta,\alpha}^+ \otimes \hat{t}_{a,\alpha} \\ & \otimes \hat{G}_{a,b}^- \otimes \hat{t}_{b,\beta} + \hat{t}_{\beta,b} \otimes \hat{G}_{b,a}^+ \otimes \hat{t}_{a,\alpha} \otimes \hat{G}_{\alpha,\beta}^- - \hat{G}_{\beta,a}^+ \otimes \hat{t}_{a,\alpha} \\ & \otimes \hat{G}_{\alpha,b}^- \otimes \hat{t}_{b,\beta}], \end{aligned} \quad (3)$$

where the trace is a sum over the channels in real space (see Fig. 2) and over electron and hole components of the Nambu representation. The symbol \otimes denotes convolution over time variables and the dependence on time variables is implicit in Eq. (3). The notations α_n, β_n are used for the counterparts in the superconductor of the tight-binding sites a_n and b_n at the interfaces of electrodes $N_{a,b}$ (see Fig. 2). The notation $\hat{g}_{i,j}$ corresponds to the Nambu Green's function of electrodes isolated from each other, while the notations $\hat{G}_{i,j}^+$ and $\hat{G}_{i,j}^-$ are used for electrodes connected to each other by arbitrary interface transparencies. For instance one has the following for the Keldysh Green's function $G_{i,j}^+(t_1, t_2)$:

$$\hat{G}_{i,j}^+(t_1, t_2) = i \begin{pmatrix} \langle c_{j,\uparrow}^+(t_2) c_{i,\uparrow}(t_1) \rangle & \langle c_{j,\downarrow}(t_2) c_{i,\uparrow}(t_1) \rangle \\ \langle c_{j,\uparrow}^+(t_2) c_{i,\downarrow}^+(t_1) \rangle & \langle c_{j,\downarrow}(t_2) c_{i,\downarrow}^+(t_1) \rangle \end{pmatrix}. \quad (4)$$

In Eq. (3), $\hat{t}_{i,j}$ denotes the Nambu hopping amplitude from i to j :

$$\hat{t}_{i,j} = \begin{pmatrix} |t_{i,j}| & 0 \\ 0 & -|t_{i,j}| \end{pmatrix}. \quad (5)$$

Based on a standard description,²⁰ we suppose that propagation in the normal electrodes $N_{a,b}$ is local, as for a vanishingly small phase coherence length. Some processes that delocalize in the direction parallel to the interfaces²¹ are not accounted for. Then the multichannel contact on Fig. 2 can be replaced by a single channel contact, and this is why we use in Eq. (3) the notations a, α, β, b instead of a_n, α_n, β_n and b_n [see Fig. 2(a)], and average over the Fermi phase factor $k_F R$ entering nonlocal propagation in the superconductor.

To discuss both highly transparent interfaces and an arbitrary distance between the contacts, we solve the Dyson equation of the form

$$\hat{A} \hat{G}_{\alpha,\beta} = \hat{g}_{\alpha,\beta} + \hat{X}_{\alpha,\beta} \hat{G}_{\beta,\beta}, \quad (6)$$

$$\hat{B} \hat{G}_{\beta,\beta} = \hat{g}_{\beta,\beta} + \hat{X}_{\beta,\alpha} \hat{G}_{\alpha,\beta}, \quad (7)$$

with

$$\hat{A} = \hat{I} - \hat{g}_{\alpha,\alpha} \hat{t}_{\alpha,a} \hat{g}_{a,a} \hat{t}_{a,\alpha}, \quad (8)$$

$$\hat{B} = \hat{I} - \hat{g}_{\beta,\beta} \hat{t}_{\beta,b} \hat{g}_{b,b} \hat{t}_{b,\beta}, \quad (9)$$

$$\hat{X}_{\alpha,\beta} = \hat{g}_{\alpha,\beta} \hat{t}_{\beta,b} \hat{g}_{b,b} \hat{t}_{b,\beta}, \quad (10)$$

$$\hat{X}_{\beta,\alpha} = \hat{g}_{\beta,\alpha} \hat{t}_{\alpha,a} \hat{g}_{a,a} \hat{t}_{a,\alpha}. \quad (11)$$

Then we have

$$\hat{G}_{\alpha,\beta} = \hat{Y}^{-1} \hat{g}_{\alpha,\beta} + \hat{Y}^{-1} \hat{X}_{\alpha,\beta} \hat{B}^{-1} \hat{g}_{\beta,\beta}, \quad (12)$$

$$\hat{G}_{\beta,\beta} = \hat{B}^{-1} \hat{g}_{\beta,\beta} + \hat{B}^{-1} \hat{X}_{\beta,\alpha} \hat{G}_{\alpha,\beta}, \quad (13)$$

where we used the notation

$$\hat{Y} = \hat{A} - \hat{X}_{\alpha,\beta} \hat{B}^{-1} \hat{X}_{\beta,\alpha}. \quad (14)$$

The Keldysh Green's functions $\hat{G}_{a,\alpha}^{+-}(\omega)$ and $\hat{G}_{\alpha,a}^{+-}(\omega)$ are next obtained from the Dyson-Keldysh equations³¹⁻³³

$$\begin{aligned} \hat{G}_{a,\alpha}^{+-}(\omega) = & [\hat{I} + \hat{G}_{a,\alpha}^R(\omega) \hat{t}_{\alpha,a}] \hat{g}_{a,\alpha}^{+-}(\omega) \hat{t}_{a,\alpha} \hat{G}_{\alpha,\alpha}^A(\omega) \\ & + \hat{G}_{a,\beta}^R(\omega) \hat{t}_{\beta,b} \hat{g}_{b,b}^{+-}(\omega) \hat{t}_{b,\beta} \hat{G}_{\beta,\alpha}^A(\omega), \end{aligned} \quad (15)$$

$$\begin{aligned} \hat{G}_{\alpha,a}^{+-}(\omega) = & \hat{G}_{\alpha,\alpha}^R(\omega) \hat{t}_{\alpha,a} \hat{g}_{a,\alpha}^{+-}(\omega) [\hat{I} + \hat{t}_{a,\alpha} \hat{G}_{\alpha,\alpha}^A(\omega)] \\ & + \hat{G}_{\alpha,\beta}^R(\omega) \hat{t}_{\beta,b} \hat{g}_{b,b}^{+-}(\omega) \hat{t}_{b,\beta} \hat{G}_{\beta,\alpha}^A(\omega), \end{aligned} \quad (16)$$

where we Fourier transformed from time t to frequency ω . Note that ω is conjugate to the time difference in Eq. (1), and thus we consider zero frequency noise. The notations $\hat{G}_{i,j}^{A,R}(\omega)$ are used for the advanced and retarded fully dressed Green's functions connecting i and j at frequency ω .

The method discussed here allows us to treat an arbitrary distance between the normal electrodes and contains all information about quantum interference effects,³⁴ unlike quasiclassics.³⁵ We did not find qualitative changes of the crossed conductance and of the sign of noise cross-correlations when crossing over from $R \gtrsim \xi$ to $R \lesssim \xi$ within the Green's function approach and therefore we present the results only for $R \gtrsim \xi$, in which case we recovered for the crossed conductance the behavior of Refs. 20, 23, and 24.

B. Blonder-Tinkham-Klapwijk (BTK) approach to noise cross-correlations

The Blonder-Tinkham-Klapwijk³⁶ (BTK) approach was previously applied to nonlocal transport,²⁴ i.e., computing the current voltage characteristics in the different leads (see also Ref. 16). Here it is extended to address noise cross-correlations. Considering a one-dimensional (1D) $N_a S N_b$ structure [see Fig. 2(b)], three regions are connected to each other: (i) Normal electrode N_a at coordinate $x < 0$; (ii) superconducting region S for $0 < x < R$, and (iii) normal electrode N_b for $x > R$.

The two-component wave-function in electrode N_a takes the form

$$\begin{aligned} \psi_a(x) = & \begin{pmatrix} 1 \\ 0 \end{pmatrix} \exp(ik_F x) + s_{aa}^{eh} \begin{pmatrix} 0 \\ 1 \end{pmatrix} \exp(ik_F x) \\ & + s_{aa}^{ee} \begin{pmatrix} 1 \\ 0 \end{pmatrix} \exp(-ik_F x). \end{aligned} \quad (17)$$

The two-component wave-function in electrode S takes the form

$$\begin{aligned} \psi_S(x) = & c \begin{pmatrix} u_0 \\ v_0 \end{pmatrix} \exp(ik_F x) \exp(-x/\xi) + d \begin{pmatrix} v_0 \\ u_0 \end{pmatrix} \exp(-ik_F x) \\ & \times \exp(-x/\xi) + c' \begin{pmatrix} u_0 \\ v_0 \end{pmatrix} \exp[-ik_F(x-R)] \\ & \times \exp[(x-R)/\xi] + d' \begin{pmatrix} v_0 \\ u_0 \end{pmatrix} \exp[ik_F(x-R)] \\ & \times \exp[(x-R)/\xi], \end{aligned} \quad (18)$$

and in electrode N_b it is given by

$$\psi_b(x) = s_{ab}^{eh} \begin{pmatrix} 0 \\ 1 \end{pmatrix} \exp[-ik_F(x-R)] + s_{ab}^{ee} \begin{pmatrix} 1 \\ 0 \end{pmatrix} \exp[ik_F(x-R)].$$

The amplitudes are specified by matching the electron and hole wave functions and their derivatives at both boundaries. They describe Andreev reflection (s_{aa}^{eh}), normal reflection (s_{aa}^{ee}), crossed Andreev reflection (s_{ab}^{eh}) and elastic cotunneling (s_{ab}^{ee}), as well as transmission in the superconductor with or without branch crossing of evanescent states localized at the left or right interfaces (coefficients c , d , c' , and d'). Under standard assumptions, the zero frequency noise cross-correlations (the time integral of the real time crossed correlator) are given by^{18,19} $S_{a,b} = \sum_{k,l} S_{a,b}^{(k,l)}$, where k, l label electrodes N_a and N_b , and where

$$\begin{aligned} S_{a,b}^{(k,l)} = & \int_0^{2\pi} \frac{d(k_F R)}{2\pi} \sum_{\alpha,\beta,\gamma,\delta \in \{e,h\}} \frac{q_\alpha q_\beta}{h} \\ & \times \int d\omega A_{k\gamma,l\delta}(a\alpha) A_{l\delta,k\gamma}(b\beta) f_{k\gamma}(1-f_{l\delta}), \end{aligned} \quad (19)$$

where Greek indices denotes the nature (e for electrons, h for holes) of the incoming or outgoing particles with their associated charges q_α , while Latin symbols l, k identify the leads. $f_{k\gamma}$ is a Fermi function for particles of type γ in reservoir k at energy $\hbar\omega$. The matrix

$$A_{k\gamma,l\delta}(i\alpha) \equiv \delta_{ik} \delta_{il} \delta_{\alpha\gamma} \delta_{\alpha\delta} - s_{ik}^{\alpha\gamma\dagger} s_{il}^{\alpha\delta}, \quad (20)$$

enters the definition of the current operator, and contains all the information about the scattering process which were described above.

Note that the noise cross-correlations in Eq. (19) are averaged over the Fermi phase factor $k_F R$ accumulated while traversing the superconductor, which is a standard procedure for evaluating nonlocal transport through a superconductor.²⁰

C. Comparison between the two methods

We carried out systematically all calculations with the two approaches (microscopic Green's functions and BTK) in or-

der to determine which are the generic feature of the noise cross-correlation spectra. We find such model-independent variations of the noise cross-correlation spectra in the limit of small interface transparencies³⁰ and for highly transparent interfaces. The two approaches do not coincide at the cross-over between small and large interface transparencies because different assumptions are made about the geometry. We complement these numerical results by an explanation from the Antram-Datta¹⁸ noise cross-correlation formula of why noise cross-correlations are positive for highly transparent interfaces and at small bias.

For microscopic Green's functions we calculate the non local conductance and the noise cross-correlations of a single channel contacts, in the spirit of the approach by Cuevas *et al.*³³ for a S-S break junction, and averaged over the microscopic Fermi phase factors. The electrons (or pairs of electrons) tunneling through such weak links have to reduce in size down to atomic dimensions in order to traverse the junction, resulting as in optics in diffraction. In this approach, the tunneling Hamiltonian transfers electrons from one point in the normal metal lead to one point in the superconductor. The contribution of wave functions from all momenta in the normal metal are extracted to tunnel into a point in the superconductor therefore transferring to all momenta states in the latter (and vice versa). On the opposite, in the 1D BTK model, a single (transverse) mode on the normal side is converted into a single mode in the superconductor. Diffraction effects are absent for the one-dimensional BTK model. As an example, for perfect interfaces, a hole cannot be forward-scattered in the 1D BTK model. A natural interpretation of this effect for the 1D BTK model²³ is momentum conservation for perfect transmission.

III. RESULTS

A. Half-metal–superconductor–half-metal structures

The dominant transmission channel can be controlled by the relative spin orientation in the case of half-metals (containing only majority spin electrons). More precisely, as mentioned in the Introduction, two processes contribute to the nonlocal conductance in this case (see Fig. 1): Elastic cotunneling (transmission of a spin-up electron from electrode F_b as a spin-up electron in electrode F_a) and crossed Andreev reflection (transmission of a spin-up electron from electrode F_b as a hole in the spin-down band in electrode F_a with a pair left in the superconductor). The dominant nonlocal transport channel can be selected by the relative spin orientation of half-metals: elastic cotunneling in the parallel (P) alignment and crossed Andreev reflection in the antiparallel (AP) alignment.

The resulting noise cross-correlations are shown on Fig. 3 for half-metals in the parallel [Fig. 3(a)] and antiparallel [Fig. 3(b)] alignments and for different values of the transmission coefficients ranging from tunnel to highly transparent interfaces. We obtain a characteristic sign of noise cross-correlations for the two spin orientations (negative cross-correlations for elastic cotunneling, and positive cross-correlations for crossed Andreev reflection), and a characteristic dependence on the voltage V_b at fixed V_a .

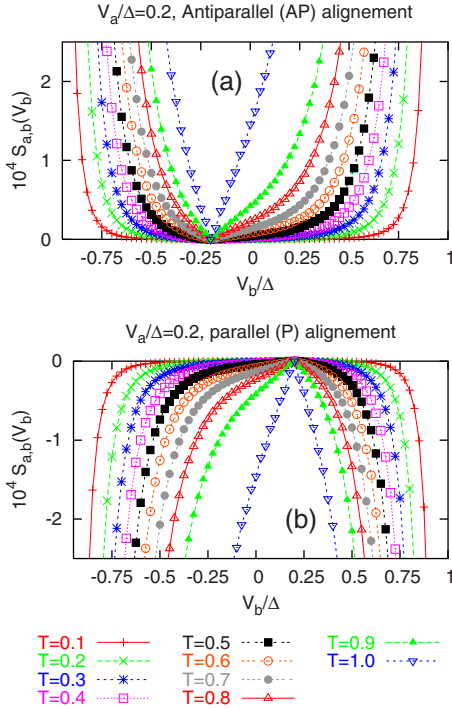


FIG. 3. (Color online) Noise $S_{a,b}(eV_b/\Delta)$ of a $F_a S F_b$ three-terminal structure with ferromagnetic electrodes F_a and F_b with (a) antiparallel spin orientations and with (b) parallel spin orientations, for interface transparencies ranging from $T=0.1$ to $T=1$. The voltage on electrode F_a is fixed to $V_a/\Delta=0.2$. The distance R between the contacts is such that $\exp(-R/\xi_0)=10^{-2}$, with ξ_0 the BCS coherence length at zero energy. The dependence of the coherence length on energy is supposed to have the BCS form for a ballistic superconductor. The noise spectra on this figure are obtained from microscopic Green's functions.

For each setup (antiparallel or parallel alignment), there is a special value of voltage where the noise cross-correlations vanish. For instance, the vanishing of the noise cross-correlations occurs at $V_b=-V_a$ for the antiparallel configuration. For half-metals, a (singlet) Cooper pair cannot be transmitted as a whole in the right or left lead because of the opposite spin orientation of the two leads. The two electrons of a Cooper pairs have then to end up into two electrodes with different chemical potentials, and one has then determine whether the incoming and outgoing states are available (see Fig. 4). For the value of voltages $V_b=-V_a$, electrons with opposite energies with respect to the superconducting chemical potential are not available, and the same is true for pairs of holes with opposite energies. Therefore, the cross-correlations vanish for this value of voltage, but they increase gradually for voltages $V_b>-V_a$ or $V_b<-V_a$ as Pauli blocking effects disappear.

B. Normal metal–superconductor–normal metal structures

We consider now a one-dimensional $N_a S N_b$ structure within the Green's function approach as well as within the one-dimensional BTK approach. The dependence of the noise cross-correlations $S_{a,b}(V_a, V_b)$ on eV_b/Δ for a fixed

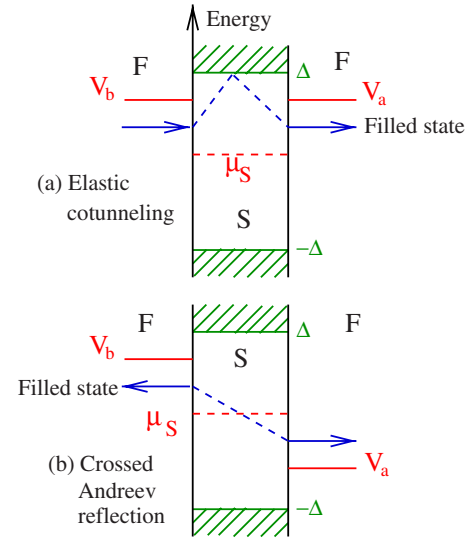


FIG. 4. (Color online) Pauli blocking as exemplified in (a) electron-cotunneling setup and (b) for a crossed Andreev reflection setup. For (a), an electron incoming from F_b cannot be transmitted in F_a due to Pauli blocking for $V_b=V_a$. For (b) a pair from the superconductor cannot split in electrodes F_a and F_b if $V_b=-V_a$.

eV_a/Δ at zero temperature is shown in Figs. 5 and 6, for tunnel interfaces to highly transparent interfaces. For the BTK approach, the scattering coefficients s_{aa}^{ee} , s_{aa}^{eh} , s_{ab}^{eh} , and s_{ab}^{ee} are parametrized by a single interface parameter z (for this symmetric system), $z \equiv 2mH/\hbar^2 k_F$, where m is the band mass, and H is the strength of the delta potential at the interface. The parameter z is related to the transmission probability in the normal state

$$z^2 = \frac{1 - T_0}{T_0}. \quad (21)$$

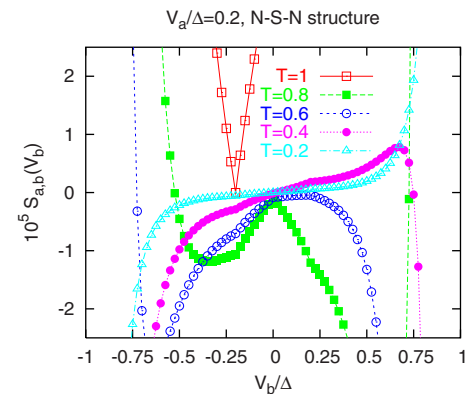


FIG. 5. (Color online) Noise $S_{a,b}(eV_b/\Delta)$ of a $N_a S N_b$ three-terminal structure with normal electrodes N_a and N_b for moderate and high interface transparencies (normal transmissions $T=0.2, 0.4, 0.6, 0.8, 1$), within microscopic Green's functions. The tunnel limit (Ref. 30) with $S_{a,b}(eV_b/\Delta)$ linear in V_b in the window $-V_a < V_b < V_a$ is recovered for small T . The distance R between the contacts is such that $\exp(-R/\xi_0)=10^{-2}$, with ξ_0 the BCS coherence length at zero energy.

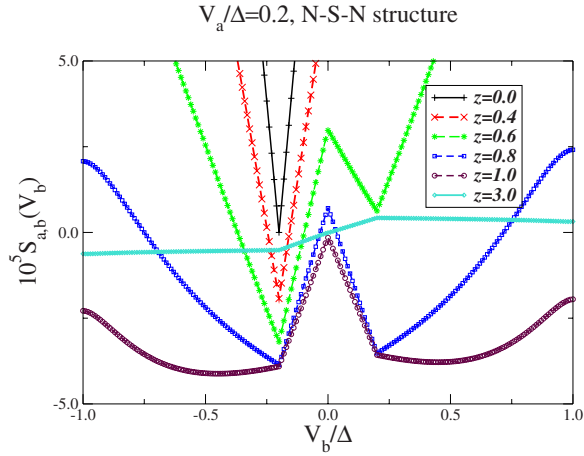


FIG. 6. (Color online) Noise $S_{a,b}(eV_b/\Delta)$ of a N_aSN_b three-terminal structure with normal electrodes N_a and N_b from transparent ($z=0.0$) to tunneling ($z=3.0$) interfaces, from the BTK approach. The tunnel behavior (Ref. 30) with $S_{a,b}(eV_b/\Delta)$ linear in V_b in the window $-V_a < V_b < V_a$ is recovered for large z in the tunnel limit. The distance R between the contacts is such that $\exp(-R/\xi_0)=10^{-2}$, with ξ_0 the BCS coherence length at zero energy.

The expected Bignon *et al.*³⁰ tunnel limit for noise cross-correlations is recovered in both cases. In this case, the noise cross-correlations vary almost linearly if the voltage V_b is smaller than V_a (in absolute value) are recovered for small interface transparencies, in both plots. In the other limiting case of high transparencies, the overall shape of the curves is of an inverted pyramid with its apex at $V_b=-V_a$. As the transparency is increased the base of the pyramid enlarges, and the height decreases. Similar predictions are obtained in the two approaches both in the limits of small and large interface transparencies.

C. Interpretation

For high interface transparencies, it is well established^{20,23,24} that the crossed conductance is *negative*, with the same sign as normal electron transmission from one electrode to the other across the superconductor.

Let us now consider noise crossed correlations. We show that positive noise correlations are expected from the Anatan-Datta¹⁸ noise formula. We focus on the case of a small applied voltage $eV_b \ll \Delta$. First if k and l in Eq. (19) both belong to the same electrode N_a we find

$$A_{a\gamma,a\delta}(a\alpha)A_{a\delta,a\gamma}(b\beta) = \quad (22)$$

$$(\delta_{\alpha,\gamma}\delta_{\alpha,\delta} - \bar{s}_{a\gamma,a\alpha}s_{a\alpha,a\delta})(-\bar{s}_{a\delta,b\beta}s_{b\beta,a\gamma}). \quad (23)$$

At zero temperature, the terms containing $\delta_{\alpha,\gamma}\delta_{\alpha,\delta}$ do not contribute to noise cross-correlations because of the Fermi occupation factors in Eq. (19). For high transparencies, the term $\bar{s}_{a\gamma,a\alpha}s_{a\alpha,a\delta}$ encodes local Andreev reflection changing electrons into holes, with therefore $\alpha=-\gamma=-\delta$. Taking into account the four s -matrix coefficients and the prefactor containing the sign of the transmitted carriers, we deduce that

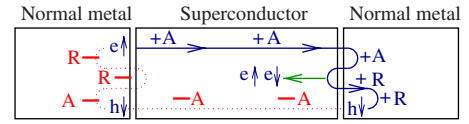


FIG. 7. (Color online) Schematic representation of the process contributing to the noise cross-correlations of a N_aSN_b structure. This process in noise cross-correlations corresponds to crossed Andreev reflection: Propagation forward in time of an electron from the left normal metal converted as a hole in the right normal metal with a pair transmitted in the superconductor, and the reverse process backward in time. Propagation forward (backward) in time are denoted by “+” (“-”) on the figure and by solid blue (dashed red) lines. We have shown on the figure the pair transmitted inside the superconductor for propagation forward in time, but, for clarity, we have not represented the corresponding process for propagation backward in time. Similarly we have shown the “advanced” (A) and “retarded” (R) labels for forward propagation in time.

this contribution to noise cross-correlation is vanishingly small. It can be shown by similar arguments that the term in $S_{a,b}^{(k,l)}$ with k and l labeling the different electrodes N_a and N_b respectively leads to positive noise cross-correlations for high interface transparencies, in agreement with Fig. 6. More precisely, in terms of scattering matrices, advanced and retarded propagations correspond to the elements of the scattering matrix s or to their complex conjugate, respectively. To the advanced and retarded labels are added here the labels encoding propagation forward or backward in time for the two branches of the Keldysh contour (see Sec. II A). Let us consider the term in $S_{a,b}^{(k,l)}$ with k and l labeling the different electrodes N_a and N_b , respectively. We deduce that, for this term, propagation forward in time is the product of an advanced nonlocal propagation from N_b to N_a , and a retarded local Andreev process at the interface SN_a . Combining the advanced and retarded terms, propagation forward in time has the net result of changing a spin-up electron from electrode N_a as a hole in the spin-down band in electrode N_b , with a pair left in the superconductor (as shown on Fig. 7), which corresponds to crossed Andreev reflection with positive noise crossed correlations (see Fig. 6). Pauli blocking is the same as for crossed Andreev reflection in a F_aSF_b structure in the antiparallel alignment. This picture holds for highly transparent interfaces at low energy.

IV. CONSEQUENCES FOR INTERACTIONS IN THE LEADS (PHENOMENOLOGICAL APPROACH)

Before concluding, we discuss briefly the inclusion of Coulomb interactions within the (one-dimensional) leads connected to the superconductor. In normal metal junctions, it is known³⁷ that electron-electron interactions change qualitatively the current voltage characteristics. Such Luttinger liquid behavior can be approached from the strong interaction limit, or alternatively from the weak interaction limit.^{38,39} In the latter, a perturbative renormalization group (RG) scheme was used to derive the renormalized scattering matrix coefficients. The interaction-induced dependence of the transmission probability on energy ω reads³⁹

$$T(\omega) = \frac{T_0 \left| \frac{\omega}{D_0} \right|^\alpha}{1 - T_0 \left(1 - \left| \frac{\omega}{D_0} \right|^\alpha \right)}, \quad (24)$$

where T_0 is the transparency in the absence of interaction, $0 < \alpha < 1$ quantifies the electron-electron interaction strength ($\alpha=0$ corresponds to no interactions), and D_0 is a high-energy cutoff determined by the energy bandwidth of the electronic states.

For normal metal–superconductor interfaces, this approach was adapted^{40,41} to predict that electron-electron interactions induce a suppression of the Andreev conductance with a nonideal transparency. However, the Andreev conductance remains unaffected by interactions for a purely transparent NS interface.

For the microscopic Green’s function approach of a three terminal N_aSN_b device, the bare transmission amplitude is thus replaced by its energy dependent value in order to obtain the noise cross correlations in the presence of interactions in the leads.

For the BTK approach, we follow the phenomenological treatment of Ref. 41, which amounts to replacing T_0 by $T(\omega)$ to account for the presence of interactions. The interaction parameter is changed to $z \rightarrow z_{ee}$:

$$z_{ee}^2 = \left| \frac{\omega}{D_0} \right|^{-\alpha} \frac{1 - T_0}{T_0} = \left| \frac{\omega}{D_0} \right|^{-\alpha} z^2. \quad (25)$$

When $z=0$ (i.e., $T_0=1$), the result $z_{e-e}=0$ implies that for a transparent interface electron-electron interactions have no effect on electronic transport.^{40,41} In the BTK approach z_{ee} is simply inserted in the expression for the scattering matrix coefficients, and the noise cross correlations are computed subsequently. We discuss briefly in the conclusion the limitations of these approaches (for the Green’s function and the BTK situation).

In Fig. 8(a) [Fig. 8(b)] the parameter α is gradually switched on to the full interaction value ($\alpha=1$) for the Green’s function calculation (for the BTK approach).

For almost transparent contacts (Fig. 9, left panel) we obtain a change from completely positive crossed correlations throughout the range to alternating between negative and positive as α is increased. The weak interactions results are analogous to their noninteracting counterparts: Single valley at $V_b = -V_a$. However, for strong interactions two valleys are located at $V_b = \pm V_a$. Further increase of interactions leads to a gradual smoothing of these features, eventually leading to the result for tunnel interfaces.³⁰

This is in contrast with the case of semitransparent contacts wherein noise cross-correlations which are uniformly negative (as in Fig. 9, right panel) turn positive as interactions are increased in the positive voltage range. Indeed, for this situation, interactions change a transparent contact into a tunneling contact.

V. CONCLUSIONS

Experiments on nonlocal Andreev reflection⁵⁻⁷ have already been achieved, and they have generated a lot of excite-

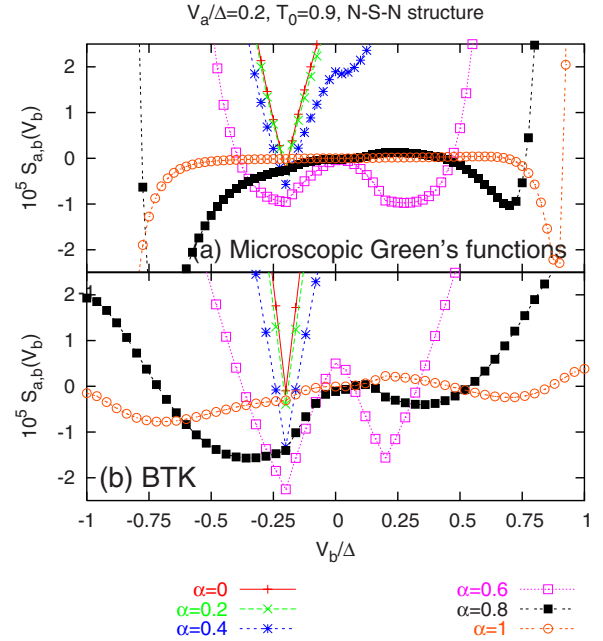


FIG. 8. (Color online) Noise $S_{a,b}(eV_b/\Delta)$ of a N_aSN_b three-terminal structure with normal electrodes N_a and N_b , for an interface transparency $T=1$ and an interaction parameter α ranging from 0 to 1. We use $D_0/\Delta=100$ for the parameter D_0 in Eq. (25). (a) and (b) correspond to microscopic Green’s functions and to the BTK approach respectively. The distance R between the contacts is such that $\exp(-R/\xi_0)=10^{-2}$, with ξ_0 the BCS coherence length at zero energy.

ment in the mesoscopic physics community. Noise cross-correlation experiments in normal metal–superconducting hybrid structures are the next on the list and experiments are under way. Such experiments could allow to observe the splitting of Cooper pairs from a superconductor into two distinct normal metal leads.

This would constitute a milestone toward probing entanglement in the context of nanophysics. A renewed theoretical interest into such questions, taking into account experimental constraints (the separation between contacts is large compared to the superconducting coherence length) is simply warranted.

In the beginning of this work, we computed the noise cross-correlation spectra as a function of voltage with varying interface transparencies for half-metal–superconductor–half-metal systems. For oppositely polarized half-metals noise cross-correlations are positive because crossed Andreev reflection is then the only possible channel of nonlocal transport. Crossed Andreev reflection leads to positive cross-correlations as electron and holes detected at separate electrodes arise from the same Cooper pair in the superconductor. However, for half-metals polarized in the parallel alignment, cross-correlations are negative because elastic cotunneling is the only means of transport. Elastic cotunneling leads to negative cross-correlation since electrons detected at the separate electrodes do not share any information. These results, which display the physics of Pauli Blocking, have an obvious interpretation in the tunneling limit. When the interface transmission is increased, we find that the overall sign

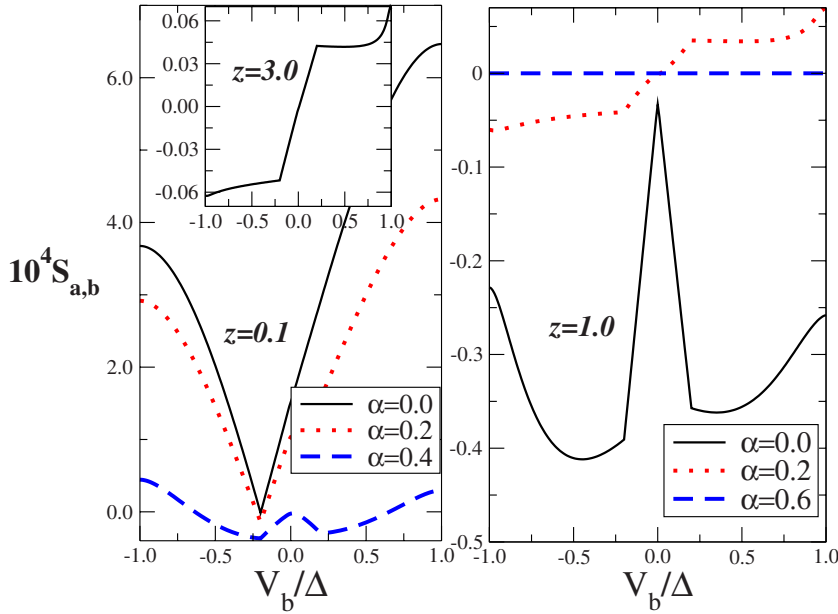


FIG. 9. (Color online) Same as Fig. 8 but with $z=0.1$ (almost transparent) while the right panel is for $z=1.0$ (semitransparent). In the inset of the left panel the plot for the tunneling limit coincides with that of Ref. 30 (linear behavior in between $-V_a < V_b < V_a$). The distance R between the contacts is such that $\exp(-R/\xi_0) = 10^{-2}$, with ξ_0 the BCS coherence length at zero energy.

of the noise correlations is unchanged. However, both for the parallel and antiparallel configuration, the amplitude of noise correlations are much more sensitive to the applied voltage, and the slope (in absolute value) around the vanishing of such correlations is increased.

But the most important part of this work concerns the results for normal metal leads, which are more accessible experimentally, but for which the splitting of Cooper pair cannot be achieved by projecting the spin. As a first check, we recover the tunneling limit results,³⁰ where the sign of cross correlations goes from positive to negative by varying the voltages attributed to each lead, and thus favoring cross Andreev processes or electron cotunneling processes. As the transparency is gradually increased, we observe a crossover to positive correlations. This result is especially robust close to ideal transparency, which constitutes the main result of this paper. This is especially surprising in the light of previous work on the nonlocal conductance.

We conclude that a negative crossed conductance is compatible with positive noise cross-correlations for highly transparent interfaces in N_aSN_b structures and this is a consequence of the different underlying process which contribute to the noise and in the nonlocal conductance. For the noise cross-correlations, an electron from N_b is converted into a hole in N_a with a pair transmitted in the superconductor, as in nonlocal (cross) Andreev reflection. For the nonlocal conductance, a pair of electrons from N_b tunnels through the superconductor into electrode N_a effectively in the form of two-electron cotunneling. This means that for transparent interfaces, the negative crossed conductance is not expected to be a signature of entanglement whereas the positive noise crossed correlation signal provides an evidence for the presence of entangled electrons between the two leads.

We found it informative to address the issue of interactions, if the normal metal leads are one dimensional. Rather than providing a detailed derivation of the renormalization procedure for this system with two interfaces, we chose a

phenomenological approach⁴¹ which “only” renormalizes the hopping amplitudes or interaction parameters at the two interfaces, rather than treating the two leads system as a whole. We find that for near ideal interfaces, interactions reduce the amplitude of the positive noise cross correlation signal and can even reverse its sign for strong interactions. For intermediate to low interfaces, upon renormalization the result coincides with the tunneling limit as it should be. Granted, these constitute preliminary results, because in particular the renormalization of the transmission phase is not described rigorously by renormalization group equations, as in Refs. 40 and 42. However, as far as the current for a single interface is concerned, results from the exact works are reproduced with this phenomenological approach, as seen from Refs. 41 and 42. One could expect that the separation between the two normal metal–superconductor interfaces could complicate things (compared to a single interface), but many round trips between the two interfaces are prohibited by our assumption of a large contact separation (compared to the coherence length). Moreover, for single interfaces, the renormalization of the Andreev reflection *phase* is predicted⁴⁰ to affect only transport through geometries containing two superconductors (Josephson effect). Nevertheless, the renormalization treatment of the full two interface problem would constitute an extension of the present work.

Effects associated with one dimensional leads could be experimentally probed when connecting a superconductor to carbon nanotube wires, which could exhibit Luttinger liquid behavior. Experiments with a single nanotube split into two leads by an overlapping superconducting contact have been recently achieved in Ref. 43.

A connection between the work of Ref. 44 and the present situation with interacting one-dimensional leads can be envisioned, due to the fact that the physics of dynamical Coulomb blockade³⁷ is intimately tied to the physics of tunneling between Luttinger liquids (excitation of “many” bosonic modes during an electron tunneling event). Further work dealing with the finite frequency spectrum of noise cross-

correlations, possibly in the presence of such interactions⁴⁴ would constitute a relevant extension of this work.

ACKNOWLEDGMENTS

R.M. acknowledges a fruitful discussion with D. Feinberg

on the BTK approach to nonlocal transport. T.M. acknowledges support from ANR grant “Molspintronics” from the French ministry of research. R.M. acknowledges support from ANR grant “Elec-EPR” from the French Ministry of research.

-
- ¹J. M. Byers and M. E. Flatté, *Phys. Rev. Lett.* **74**, 306 (1995).
²G. B. Lesovik, T. Martin, and G. Blatter, *Eur. Phys. J. B* **24**, 287 (2001); N. M. Chtchelkatchev, G. Blatter, G. B. Lesovik, and T. Martin, *Phys. Rev. B* **66**, 161320(R) (2002).
³M. S. Choi, C. Bruder, and D. Loss, *Phys. Rev. B* **62**, 13569 (2000); P. Recher, E. V. Sukhorukov, and D. Loss, *Phys. Rev. B* **63**, 165314 (2001).
⁴G. Deutscher and D. Feinberg, *Appl. Phys. Lett.* **76**, 487 (2000).
⁵D. Beckmann, H. B. Weber, and H. v. Löhneysen, *Phys. Rev. Lett.* **93**, 197003 (2004).
⁶S. Russo, M. Kroug, T. M. Klapwijk, and A. F. Morpurgo, *Phys. Rev. Lett.* **95**, 027002 (2005).
⁷P. Cadden-Zimansky and V. Chandrasekhar, *Phys. Rev. Lett.* **97**, 237003 (2006).
⁸B.-R. Choi, A. E. Hansen, T. Kontos, C. Hoffmann, S. Oberholzer, W. Belzig, C. Schönberger, T. Akazaki, and H. Takayanagi, *Phys. Rev. B* **72**, 024501 (2005); P. Roche, H. Perrin, D. C. Glatli, H. Takayanagi, and T. Akazaki, *Physica C* **352**, 73 (2001).
⁹X. Jehl, M. Sanquer, R. Calemczuk, and D. Mailly, *Nature (London)* **405**, 50 (2000); A. A. Kozhevnikov, R. J. Schoelkopf, and D. E. Prober, *Phys. Rev. Lett.* **84**, 3398 (2000).
¹⁰N. K. Allsopp, V. C. Hui, C. J. Lambert, and S. J. Robinson, *J. Phys.: Condens. Matter* **6**, 10475 (1994); C. J. Lambert and R. Raimondi, *J. Phys.: Condens. Matter* **10**, 901 (1998).
¹¹F. J. Jedema, B. J. van Wees, B. H. Hoving, A. T. Filip, and T. M. Klapwijk, *Phys. Rev. B* **60**, 16549 (1999); B. J. van Wees and H. Takayanagi, in *Mesoscopic Electron Transport*, edited by L. Sohn, L. Kouwenhoven, and G. Schön, NATO Advanced Study Institute, Series E: Applied Science (Kluwer Academic, Dordrecht, 1996), Vol. 345.
¹²G. Falci, D. Feinberg, and F. Hekking, *Europhys. Lett.* **54**, 255 (2001).
¹³P. Samuelsson and M. Büttiker, *Phys. Rev. Lett.* **89**, 046601 (2002); *Phys. Rev. B* **66**, 201306(R) (2002); P. Samuelsson, E. V. Sukhorukov, and M. Büttiker, *Phys. Rev. Lett.* **91**, 157002 (2003).
¹⁴E. Prada and F. Sols, *Eur. Phys. J. B* **40**, 379 (2004).
¹⁵P. K. Polinák, C. J. Lambert, J. Koltai, and J. Cserti, *Phys. Rev. B* **74**, 132508 (2006).
¹⁶T. Yamashita, S. Takahashi, and S. Maekawa, *Phys. Rev. B* **68**, 174504 (2003).
¹⁷D. Feinberg, *Eur. Phys. J. B* **36**, 419 (2003).
¹⁸M. P. Anantram and S. Datta, *Phys. Rev. B* **53**, 16390 (1996).
¹⁹Y. Blanter and M. Büttiker, *Phys. Rep.* **336**, 1 (2000).
²⁰R. Mélin and D. Feinberg, *Phys. Rev. B* **70**, 174509 (2004).
²¹R. Mélin, *Phys. Rev. B* **73**, 174512 (2006).
²²A. Levy Yeyati, F. S. Bergeret, A. Martín-Rodero, and T. M. Klapwijk, *Nat. Phys.* **3**, 455 (2007).
²³R. Mélin, *Phys. Rev. B* **73**, 174512 (2006); S. Duhot and R. Mélin, *Phys. Rev. B* **75**, 184531 (2007).
²⁴S. Duhot and R. Mélin, *Eur. Phys. J. B* **53**, 257 (2006).
²⁵J. P. Morten, A. Brataas, and W. Belzig, *Phys. Rev. B* **74**, 214510 (2006); J. P. Morten, D. Huertas-Hernando, A. Brataas, and W. Belzig, arXiv:cond-mat/0612197 (unpublished).
²⁶F. Taddei and R. Fazio, *Phys. Rev. B* **65**, 134522 (2002); F. Giazotto, F. Taddei, F. Beltram, and R. Fazio, *Phys. Rev. Lett.* **97**, 087001 (2006).
²⁷A. Brinkman and A. A. Golubov, *Phys. Rev. B* **74**, 214512 (2006).
²⁸T. Martin, *Phys. Lett. A* **220**, 137 (1996); J. Torrès and T. Martin, *Eur. Phys. J. B* **12**, 319 (1999); J. Torrès, T. Martin, and G. B. Lesovik, *Phys. Rev. B* **63**, 134517 (2001).
²⁹A. Cottet, W. Belzig, and C. Bruder, *Phys. Rev. Lett.* **92**, 206801 (2004); C. Texier and M. Büttiker, *Phys. Rev. B* **62**, 7454 (2000).
³⁰G. Bignon, M. Houzet, F. Pistolesi, and F. W. J. Hekking, *Europhys. Lett.* **67**, 110 (2004).
³¹C. Caroli, R. Combescot, P. Nozieres, and D. Saint-James, *J. Phys. C* **4**, 916 (1971).
³²J. C. Cuevas, A. Martín-Rodero, and A. L. Yeyati, *Phys. Rev. Lett.* **82**, 4086 (1999).
³³J. C. Cuevas, A. Martín-Rodero, and A. L. Yeyati, *Phys. Rev. B* **54**, 7366 (1996).
³⁴R. Mélin, *Phys. Rev. B* **73**, 174512 (2006); S. Duhot and R. Mélin, *Phys. Rev. B* **76**, 184503 (2007).
³⁵M. S. Kalenkov and A. D. Zaikin, *Phys. Rev. B* **75**, 172503 (2007).
³⁶G. E. Blonder, M. Tinkham, and T. M. Klapwijk, *Phys. Rev. B* **25**, 4515 (1982).
³⁷G. L. Ingold and Yu. V. Nazarov, in *Single Charge Tunneling*, edited by H. Grabert and M. H. Devoret (Plenum, New York, 1992).
³⁸M. P. A. Fisher and L. I. Glazman, in *Mesoscopic Electron Transport*, edited by L. Kouwenhoven, G. Schön, and L. Sohn, NATO Advanced Study Institute Series E: Applied Science (Kluwer Academic Publishers, Dordrecht, 1997), Vol. 345.
³⁹D. Yue, L. I. Glazman, and K. A. Matveev, *Phys. Rev. B* **49**, 1966 (1994).
⁴⁰M. Titov, M. Müller, and W. Belzig, *Phys. Rev. Lett.* **97**, 237006 (2006).
⁴¹H. T. Man, T. M. Klapwijk, and A. F. Morpurgo, arXiv:cond-mat/0504566 (unpublished).
⁴²Y. Takane and Y. Koyama, *J. Phys. Soc. Jpn.* **66**, 419 (1997).
⁴³J.-P. Cleuziou, W. Wernsdorfer, V. Bouchiat, T. Ondarcuhu, and M. Monthieux, *Nat. Nanotechnol.* **1**, 53 (2006).
⁴⁴A. L. Yeyati, A. Martín-Rodero, D. Esteve, and C. Urbina, *Phys. Rev. Lett.* **87**, 046802 (2001).